Atmos. Chem. Phys. Discuss., 12, 26207–26243, 2012
www.atmos-chem-phys-discuss.net/12/26207/2012/
doi:10.5194/acpd-12-26207-2012

Atmospheric Chemistry and Physics Discussions

CH_4 and CO distributions over tropical fires as observed by the Aura TES satellite instrument and modeled by GEOS-Chem

J. Worden[1], K. Wecht[2], C. Frankenberg[1], M. Alvarado[3], K. Bowman[1], E. Kort[1], S. Kulawik[1], M. Lee[1], V. Payne[1], and H. Worden[4]

[1]Jet Propulsion Laboratory/California Institute of Technology, Pasadena, California, USA
[2]Harvard University, Cambridge, Massachusetts, USA
[3]Atmospheric and Environmental Research, Lexington, Massachusetts, USA
[4]National Center for Atmospheric Research, Boulder, CO, USA

Received: 8 September 2012 – Accepted: 12 September 2012 – Published: 5 October 2012

Correspondence to: J. Worden (john.worden@jpl.nasa.gov)

Published by Copernicus Publications on behalf of the European Geosciences Union.

Abstract

Tropical fires represent a highly uncertain source of atmospheric methane (CH_4) because of the variability of fire emissions and the dependency of the fire CH_4 emission factors ($g\,kg^{-1}$ dry matter burned) on fuel type and combustion phase. In this paper we use new observations of CH_4 and CO in the free troposphere from the Aura Tropospheric Emission Sounder (TES) satellite instrument to place constraints on the role of tropical fire emissions versus microbial production (e.g. in wetlands and livestock) during the (October) 2006 El Nino, a time of significant peat fire emissions from Indonesia We first evaluate the global CH_4 distributions from TES using the GEOS-Chem model. We find a mean bias between the observations and model of 26.3 ppb CH_4 that is independent of latitude between 50° S and 80° N consistent with previous validation studies of TES CH_4 retrievals using aircraft measurements. The slope of the distribution of CH_4 versus CO as observed by TES and modeled by GEOS-Chem is consistent (within the TES observation error) for air parcels over the Indonesian peat fires, South America, and Africa. The CH_4 and CO distributions are correlated between $R = 0.42$ and $R = 0.46$, with these correlations primarily limited by the TES random error. Over Indonesia, the observed slope of 0.13 ($ppb\,ppb^{-1}$) ± 0.01, as compared to a modeled slop of 0.153 ($ppb\,ppb^{-1}$) ± 0.005 and an emission ratio used within the GEOS-Chem model of approximately 0.11 ($ppb\,ppb^{-1}$) indicates that most of the observed methane enhancement originated from the fire. Slopes of 0.47 ($ppb\,ppb^{-1}$) ± 0.04 and 0.44 ($ppb\,ppb^{-1}$) ± 0.03 over South America and Africa show that the methane in the observed air parcels primarily came from microbial generated emissions. Sensitivity studies using GEOS-Chem show that part of the observed correlation for the Indonesian observations and most of the observed correlations over South America and Africa are a result of transport and mixing of the fire and nearby microbial generated emissions into the observed air parcels. Differences between observed and modeled CH_4 distributions over South America and Southern Africa indicate that the magnitude of the methane emissions for this time period are inconsistent with observations even if

ACPD

12, 26207–26243, 2012

the relative distribution of fire versus biotic emissions are consistent. This study shows the potential for estimation of CH_4 emissions over tropical regions using joint satellite observations of CH_4 and CO.

1 Introduction

Atmospheric methane (CH_4) concentrations have increased nearly three-fold since pre-industrial times, largely attributable to gas exploration, coal mining, rice agriculture, waste handling, and an increased population of ruminants (Forster et al., 2007). Methane concentrations stabilized in 1999 (Rigby et al., 2008) but then began increasing again in 2007 for essentially unknown reasons. For example, the persistence of the increase between 2007 and 2012 casts doubt on earlier hypotheses of anomalous rainfall and temperature patterns as culprit (Rigby et al., 2008; Dlugokencky et al., 2009; Bloom et al., 2010; Bousquet et al., 2011).

It is now recognized that one of the most efficient methods to mitigate warming due to greenhouse gases on decadal time frames is to cut methane emissions (Shindell et al., 2012) as the warming potential for methane is 72 times higher than carbon dioxide (CO_2) on a 20 yr time horizon (e.g. Forster et al., 2007; Lelieveld et al., 1998). The dominant CH_4 sink is oxidation by OH radicals in the atmosphere, resulting in a short 9-yr lifetime (e.g. Fung et al., 1991); reducing methane emissions thus rapidly lowers its atmospheric abundance. Quantifying anthropogenic and natural methane emissions is thus critical for identifying methane emission reduction targets, verifying that these target have been met, and understanding climate/carbon cycle feedbacks, as increased warming can lead to increased high-latitude methane emissions from the soil or from biomass burning (e.g. O'Connor et al., 2010 and references therein).

Approximately half of the annual 550 $Tg\,yr^{-1}$ methane emissions are anthropogenic with the bulk of these anthropogenic emissions distributed in the northern mid-latitudes (e.g. Fung et al., 1991; Lelieveld et al., 1998; Bousquet et al., 2006). Bottom-up quantification of emissions is intrinsically more difficult for methane than for CO_2 because most

ACPD
12, 26207–26243, 2012

non-energy related CH_4 emissions are biogenic, i.e. the CH_4 is created by microbes (methanogens) in anaerobic habitats such as wetlands, landfills, agricultural soils, rice paddies, and the stomachs of ruminants. Consequently, uncertainties in natural and anthropogenic emissions can exceed 100 % (e.g. Pétron et al., 2012).

Fires, though not a dominant source of methane (e.g. Forster et al., 2007; Dlugokencky et al., 2011), represent a significant contributor to the seasonal variability of atmospheric methane (e.g. Bousquet et al., 2006). The year 2006 was a time of significant tropical peat fire emissions over Indonesia due to a strong El Niño (e.g. Page et al., 2002; Logan et al., 2008; Nassar et al., 2009; Gonzi and Palmer, 2010). For example, Carbon Monoxide emissions from these Indonesian fires for October 2006 were approximately six times larger than in October 2005 (Logan et al., 2008). Figure 1 shows the October 2006 monthly average of surface and middle tropospheric atmospheric CO concentrations from the Terra Measurement of Pollution in the Troposphere (MOPITT) satellite instrument (Worden et al., 2010; Deeter et al., 2011, 2012). The plumes from these enhanced fire emissions was also observed in the upper troposphere by the Microwave Limb Sounder (MLS) (e.g. Gonzi and Palmer, 2010). These combined observations therefore show that the strong emissions, coupled with convection resulted in nearly the whole tropospheric column over the fire being affected by the smoke plume.

Despite recent advances in quantifying the global distribution of methane emissions from space (e.g. Frankenberg et al., 2005, 2011; Crevoisier et al., 2009), challenges remain in quantifying methane emissions from fires because of the difficulty in identifying methane enhancements in smoke plumes. The surface network is also challenged to place constraints on tropical fire emissions because fires plumes are lofted into the free troposphere (e.g. Dlugokencky et al., 2009). In this paper we use new measurements of tropospheric methane the Aura TES satellite instrument (as well as TES observations of CO) to quantify the enhancement of CH_4 relative to CO over areas of tropical biomass burning during October 2006. The TES CH_4 estimates (derived from thermal infrared radiance measurements as described in Sect. 2 and Worden et al., 2012) are

ACPD
12, 26207–26243, 2012

primarily sensitive to CH_4 concentrations and variability in the free troposphere and have little sensitivity to surface variations. However, the TES estimates mostly insensitive to aerosols because aerosol optical depth is negligible at thermal wavelengths (Verma et al., 2009). In addition, tropical fire plumes are rapidly advected or convected into the free troposphere where the TES CH_4 estimates have maximum sensitivity. We use TES estimates of CH_4 and CO (e.g. Worden et al., 2004, 2012; Logan et al., 2008; Ho et al., 2009; Luo et al., 2010) to investigate correlations and to quantify the ratio of the enhancements of CH_4 and CO over tropical fires in South America, Southern Africa, and Indonesia.

2 Description of TES instrument and CH_4 estimates

The TES instrument is an infrared, high spectral resolution, Fourier Transform spectrometer covering the spectral range between 650 to 3050 cm^{-1} (15.4 to 3.3 µm) with an apodized spectral resolution of 0.1 cm^{-1} for the nadir view (Beer et al., 2001). Spectral radiances measured by TES are used to infer atmospheric profiles using a nonlinear optimal estimation algorithm that minimizes the difference between these radiances and those calculated with the equation of radiative transfer (Clough et al., 2006), subject to the constraint that the parameters are consistent with a statistical a priori description of the atmosphere (Bowman et al., 2006). TES provides a global view of tropospheric trace gas profiles including ozone, water vapor and its isotopes, carbon monoxide and methane, along with atmospheric temperature, surface temperature, surface emissivity, effective cloud top pressure, and effective cloud optical depth (Worden et al., 2004, 2012; Kulawik et al., 2006; Eldering et al., 2007).

2.1 Vertical resolution and error characterization

Details of the TES CH_4 retrieval are discussed in Worden et al. (2012). In this paper we use TES CH_4 "Version 5" profiles. In particular we use the "Lite" products available at

ACPD
12, 26207–26243, 2012

http://tes.jpl.nasa.gov/data in which the TES Level 2 (single observation) data are (1) collected into monthly files, (2) at reduced dimensionality relative to the original TES data products, and (3) bias corrected using co-retrieved N_2O estimates. For this CH_4 retrieval, the logarithm of the volume mixing ratio (VMR) of CH_4 is simultaneously estimated along with surface temperature and the logarithm of the VMR of H_2O, HDO, and N_2O. By jointly estimating CH_4 with N_2O systematic uncertainties related to temperature, calibration, and H_2O can be mitigated in the CH_4 estimate because the vertical distribution of the sensitivities of thermal IR radiances in the 8 µm band to CH_4 and N_2O are similar (Worden et al., 2012).

TES CH_4 estimates are primarily sensitive to free tropospheric CH_4 (between approximately 850 hPa and the tropopause) with some sensitivity to the boundary layer and stratosphere as shown by a typical averaging kernel for a tropospheric CH_4 estimate in Fig. 2. The averaging kernel (left panel of Fig. 2) describes the sensitivity of the (log) CH_4 estimate to the "true" distribution of (log) CH_4. As discussed in Worden et al. (2012), we assume for the methane constraint used in the TES methane retrievals that the free-troposphere CH_4 can vary by as much as 5 % from our a priori knowledge but that CH_4 is also relatively well mixed in the troposphere. These assumptions affect both the corresponding averaging kernel (or vertical sensitivity) and the vertical distribution of uncertainties for the CH_4 estimate as shown in Fig. 2 (right panel, taken from Worden et al., 2012). The dominant uncertainty in the lower troposphere is due to errors in the TES temperature estimate. In the upper troposphere, the dominant random uncertainty is due to noise in the measured radiances.

TES CH_4 estimates have been validated using aircraft CH_4 profiles from the HIAPER Pole-to-Pole Observation (HIPPO) mission (Wecht et al., 2012) The TES data are biased by, on average, 28 ppb in the lower troposphere or approximately 1.5 %. After accounting for the vertical resolution and a priori constraint used in the retrieval (Sect. 4.1) it is found that the random uncertainty (root-mean-square difference between HIPPO and TES) is larger than the calculated uncertainty. However, this difference could result from the dependency of the TES tropospheric CH_4 estimates on stratospheric CH_4

ACPD
12, 26207–26243, 2012

variations; the HIPPO mission did not typically measure CH_4 in the stratosphere and consequently uncertainties in the assumed stratospheric CH_4 distribution can result in larger differences between the TES and HIPPO CH_4 comparisons.

2.2 CH_4 biases and errors from stratospheric sensitivity

Worden et al. (2012) shows that the vertical distribution of TES CH_4 is biased high in the upper troposphere relative to the lower troposphere by 2.8 %. However, as shown in Sect. 4, it is possible that this high bias is related in part to biases in the a priori stratospheric CH_4 distribution used for the TES CH_4 profile retrievals although it is also possible that errors in methane spectroscopy play a role (Worden et al., 2004). In order to reduce the effects of this vertically distributed bias error we average the retrieved VMRs of CH_4 and CO throughout the troposphere (i.e. from the surface to the tropopause) before comparing the TES retrievals to GEOS-Chem in Sects. 4 and 5. Note that this is not the same as a total column average because the TES data typically have little sensitivity to boundary layer CH_4 variations.

3 Description of GEOS-Chem

GEOS-Chem is a global 3-D chemical transport model driven by GEOS assimilated meteorological data from the NASA Global Modeling and Assimilation Office (GMAO) (http://acmg.seas.harvard.edu/geos/). The model is originally described by Bey et al. (2001). In this study, we run GEOS-Chem version 9-01-02 with GEOS-5 meteorological data at $2^\circ \times 2.5^\circ$ (lat,lon) horizontal resolution with 47 vertical layers. The GEOS-Chem methane simulation is developed by Wang et al. (2004) and updated by Pickett-Heaps et al. (2011). Model methane concentrations are initialized using observations from the NOAA/GMD surface network and simulated for twenty years prior to use in this study. Model methane sources include anthropogenic emissions from EDGAR 4.0 (European Commission, 2009), GFED2 biomass burning emissions (van

ACPD
12, 26207–26243, 2012

der Werf et al., 2006), and natural wetland emissions based on Kaplan (2002) and described by Pickett-Heaps et al. (2011). We compute the loss of methane from reaction with the OH radical using monthly mean 3-D OH concentration fields as discussed in Park et al. (2004). The global mean tropospheric OH concentration is 10.8 molec cm^{-3}, as constrained by methyl chloroform measurements (Prinn et al., 2005). Additional minor sinks include prescribed stratospheric loss rates (Wang et al., 2004) and soil absorption (Fung et al., 1991). The GEOS-Chem methane lifetime is 9.5 yr, consistent with the lifetime of 8.7 ± 1.3 yr reported by Denman et al. (2007).

4 Comparison of TES to GEOS-Chem global distributions

4.1 Comparison approach

In order to compare TES data to GEOS-Chem model profiles it is critical to account for the a priori constraint and vertical resolution of the TES estimate or else differences will be driven by choices in the a priori constraint instead of process errors in the model or errors in the retrieval from noise or interferences (e.g. Rodgers and Connor, 2003) If the GEOS-Chem model profile is passed through the TES instrument operator:

$$\hat{x}_{GC} = x_a + \mathbf{A}(x_{GC} - x_a) \quad (1)$$

where **A** is the TES averaging kernel matrix for the CH_4 estimate, x_a is the logarithm of the a priori profile used for the TES retrieval and x_{GC} is the logarithm of the GEOS-Chem CH_4 profile, then the difference between the TES estimate and the GEOS-Chem profile will be the uncertainties in the TES estimate which are due to noise, temperature, and radiative interferences (Eq. 3 in Worden et al., 2012) along with uncertainties in the model estimate.

We also find that errors in the GEOS-Chem stratospheric distribution of methane can strongly affect the comparison between the TES and GEOS-Chem tropospheric

ACPD
12, 26207–26243, 2012

methane distributions, even after accounting for the TES a priori constraint and averaging kernel. For example, Fig. 3 shows a comparison between a sample TES and GEOS-Chem profile over a region in South America with significant methane enhancement in the boundary layer. After the full (surface to top-of-atmosphere) TES instrument operator (Eq. 1) has been applied to the GEOS-Chem profile (black line), the GEOS-Chem estimate peaks in the upper troposphere whereas the TES profile peaks in the middle/lower troposphere. We find that the large differences between the GEOS-Chem methane distribution in the upper stratosphere and the TES a priori has a significant impact on this comparison even though the averaging kernel values at these stratospheric pressure levels are significantly smaller than the tropospheric components of the averaging kernels.

In order to mitigate this error due to large differences between the a priori and GEOS-Chem stratospheric methane distributions, the averaging kernels and model fields are first truncated near the tropopause (or 80 hPa) before applying the TES averaging kernel and a priori (the TES operator) to the GEOS-Chem fields. As a result of this operation, the vertical distribution of the GEOS-Chem estimate in the troposphere peaks lower in the troposphere (orange curve in Fig. 3) and is more comparable to the TES observations for this particular observation. Not accounting for the stratosphere in the TES/ GEOS-Chem comparison results in an error that is equivalent to the "cross-state" error described by Eqs. (17) and (18) in Worden et al. (2004). The magnitude of this cross-state error is found to be 3 ppb or less and consequently we ignore the error as it is negligible relative to the errors due to noise and temperature.

Two final retrieval and model characteristics that are empirically found to affect the TES and GEOS-Chem methane/CO comparisons are that the vertical sensitivity of the TES CH_4 and CO estimates vary differently by altitude and that uncertainties in the GEOS-Chem vertical transport can place CO or methane at incorrect altitudes. We account for these characteristics the errors due to the GEOS-Chem stratosphere and the TES vertical resolution and a priori constraint by taking the following steps: (1) we truncate the GEOS-Chem and a priori profiles, as well as the TES averaging

ACPD
12, 26207–26243, 2012

kernel at 80 hPa (or the lower stratosphere). This truncated TES instrument operator is then applied to the truncated GEOS-Chem profile (Eq. 1). (2) Both the truncated TES profile and the adjusted GEOS-Chem profile (left-most variable in Eq. 1) are then averaged by mixing ratio (not column amount) from the surface to the tropopause on the TES forward model pressure grid (Worden et al., 2012); the tropopause pressure is provided by the GMAO as part of its re-analysis fields and is included in the TES lite products used for this analysis. This same averaging (or mapping) is applied to the TES and GEOS-Chem CO estimates in order to be consistent when comparing the CH_4 and CO distributions. However the effect of stratospheric uncertainties on the CO estimates is much smaller because the averaging kernel sensitivity in the stratosphere is much lower for CO. (3) A final step is to remove data in which the stratospheric contribution to the TES estimate is found to be "large", as discussed in the next section.

4.2 Latitudinal variability of biases in TES and GEOS-Chem CH_4 comparisons

As discussed in the previous section, we find that errors in the vertical distribution of stratospheric methane in either the TES a priori or in GEOS-Chem can have a significant impact on comparisons between TES and GEOS-Chem. In this section we compare the latitudinal distribution of TES and GEOS-Chem CH_4 estimates in order to globally evaluate how errors in the stratosphere and also the tropopause height can affect GEOS-Chem and TES comparisons. Figure 4 shows the TES CH_4 estimates as compared to the GEOS-Chem values (with the averaging kernel applied) as a function of latitude. Each data point is the average of the CH_4 VMR from the surface to the tropopause. All data in which the retrieval converged and the degrees-of-freedom for signal (DOFS) are larger than 1.2 are used. The mean difference is 26.3 ppb for all data north of 50° S. This is consistent with the comparison of the TES CH_4 data to the HIPPO data, which showed a similar high bias in the TES retrievals (Wecht et al., 2012) However, the mean difference becomes larger at the southern latitudes for latitudes south of 60° S, primarily due to relatively high TES CH_4 data. These differences

ACPD
12, 26207–26243, 2012

in the southern polar region are possibly because the tropopause height from GMAO is not consistent with the effective tropopause height in the TES CH_4 a priori fields.

It is also likely that variations in differences between the TES CH_4 a priori, the GEOS-Chem CH_4 profile, and the "true" CH_4 distribution in the stratosphere also affect the results in the southern latitudes past 50° S. For example, the bottom panel of Fig. 5 shows the contribution from the stratosphere on the TES tropospheric estimate at 562 hPa. These values are calculated by summing the averaging kernel corresponding to 562 hPa for pressures lower than the average tropopause pressure (red line in top panel of Fig. 5) and dividing it by the sum of the 562 hPa averaging kernel. Differences between the TES CH_4 a priori and the "true" CH_4 distribution in the stratosphere will have a larger effect on the TES CH_4 tropospheric estimate for larger values shown in the bottom panel of Fig. 5. Lower values in the Southern Hemisphere south of 60° S are likely in error because of the lower altitude (higher pressure) tropopause heights at these latitudes. For these reasons we remove all data in subsequent comparisons for latitudes south of 50° S and if the stratospheric contribution, as described in the bottom panel if Fig. 5, is larger than 0.3.

4.3 Maps of TES and GEOS-Chem CH_4 and CO estimates

We next examine differences in the global distribution of TES and GEOS-Chem CH_4 estimates after using the quality flags and averaging approach discussed in Sects. 4.1 and 4.2. Figure 6 shows global maps of TES CH_4 tropospheric average estimates for October 2006 (Fig. 6a) along with the corresponding GEOS-Chem CH_4 distributions after applying the truncated TES instrument operator described by Eq. (1), (Fig. 6b) and the difference between the two (Fig. 6c). The individual GEOS-Chem CH_4 model values in Fig. 6b are selected by finding the closest match in time and space to the individual TES observations. Figure 7 shows global maps of CO; individual CO data used to generate this map correspond in time and space to the individual CH_4 data used to generate Fig. 6. Figure 8 shows the a priori distributions used to regularize the TES CH_4 (top panel) and CO (bottom panel) estimates. The CH_4 TES data in Fig. 6

ACPD
12, 26207–26243, 2012

have been bias corrected using the mean value of 26.3 ppb shown in Fig. 4 (bottom panel). All estimates are averaged within each 2° × 2.5° grid box, and only grid boxes with at least 4 TES observations are shown in the map. The GEOS-Chem CO values have been decreased by 19.9 ppb to account for the mean global bias between TES and GEOS-Chem CO estimates and to be consistent with previous studies indicating that TES data are effectively unbiased with respect to independent data sets (Luo et al., 2007). Unlike with the methane estimates, this bias in CO shows regional and latitudinal variations that are well above the uncertainty in the mean for a 15 degree latitudinal average. As can be seen in Figs. 1, 6 and 7, the primary differences between the TES and GEOS-Chem CH_4 estimates are typically in biomass burning outflow regions in the Southern Hemisphere or over wetlands regions in the tropical continents. However, GEOS-Chem appears to capture the methane variability over Asia and over the Indonesian peat fires as shown by the small differences between TES and GEOS-Chem over these regions. Larger mean differences (~ 10 ppb on average) between TES and GEOS-Chem are observed near the boreal forest wetland regions at high latitudes.

5 CH_4 and CO distributions in fire plumes

We next examine the role of fire emissions versus emissions from other sources (e.g. wetlands and/or livestock) in the observed methane concentrations affected by the smoke plumes from the Indonesian, South American, and African fires. For these comparisons we use the same quality flags, instrument operator, averaging, and bias correction as discussed in Sects. 4.1 and 4.2; however, each observation must now have at least 1.4 DOFS before being used as we empirically find that a profile will typically be uniformly sensitive to the CH_4 distribution from the lower troposphere through the tropopause for DOFS of 1.4 and above.

ACPD
12, 26207–26243, 2012

5.1 Indonesia fire plume

The observed distributions of CH_4 and CO for the air parcels affected by the October 2006 Indonesian fire plumes are shown in Fig. 9. All TES observations between 80° E and 130° E and 15° S to 5° N are included. The TES CH_4 and GEOS-Chem CO data have both been bias corrected as described in Sect. 4.3. The least squares derived slope for the TES data (using the data shown in Figs. 6 and 7) is 0.13 ($ppb\,ppb^{-1}$) ± 0.01 with a linear correlation coefficient (R) of 0.42. The uncertainty on this least squares derived slope is dependent on the uncertainties of the TES tropospheric CH_4 and CO tropospheric estimates that are, on average, 11.7 ppb and 3.7 ppb respectively. The root-mean-square of the difference between the TES methane and CO distribution and the solid line in Fig. 9 is 13.6 ppb indicating that a linear relationship well describes this distribution within the uncertainties of the TES data. The CH_4/CO distribution for the TES a priori are uncorrelated, as depicted in Fig. 8, indicating that the observed correlations are from the measurement and not the a priori. The corresponding CH_4/CO distribution from the GEOS-Chem model are shown as red diamonds in Fig. 9. The slope of the GEOS-Chem CH_4/CO distribution (0.153 $ppb\,ppb^{-1}$ ± 0.005 is higher than for the TES data but consistent (within 3 sigma) with the TES data (the error in the slope for the model distributions is calculated using the RMS spread of methane versus CO).

Tables 1 and 2 list the CH_4 and CO emissions used in the model for Indonesia (first column) for October 2006. The ratio of the CH_4/CO biomass burning emissions for October 2006 is 2.8/43.7 or 0.064 $Tg\,Tg^{-1}$ (Andreae and Merlet, 2001) or after accounting for molar weight, 0.112 molecules of CH_4 per CO molecule (equivalent to $ppb\,ppb^{-1}$). This emission ratio is lower than the observed ratio of 0.13 ($ppb\,ppb^{-1}$) but within 2-sigma of the calculated error. However, an updated emission ratio of 0.099 $g\,g^{-1}$ (e.g. Christian et al., 2003; van der Werf et al., 2010), or 0.173 molecules of CH_4 per CO, calculated specifically for peat fires burnt in a laboratory setting is well outside the observed slope, suggesting that the observed emissions are not just from peat fires.

ACPD
12, 26207–26243, 2012

We test to what extent transport of nearby emissions could affect our conclusions by conducting a sensitivity study in which the CH_4 emissions from biomass burning in GEOS-Chem (Table 1) are "turned-off", or set to zero, over Indonesia during the September through November 2006 time frame, while keeping CO emissions the same. The modeled slopes for this sensitivity study for the CH_4/CO distribution is 0.044 (ppb ppb^{-1}) ± 0.005 with a correlation of approximately 0.42. The lower value for the slope occurs because there is less emission of methane from other sources for the same amount of CO and also indicates that the enhanced methane observed over Indonesia results from the fire and not from other sources as this distribution does not agree with the observed distribution However, the modeled CH_4/CO distribution for the case in which there are no biomass burning emissions of methane is still correlated because co-located or nearby biotic emissions in the model are transported into the smoke plume. This correlating effect due to transport occurs even at the largely different observation (5 km × 8 km) and model (~ 250 km × 200 km) likely because the free tropospheric air parcels are sensitive to emissions over much larger spatial scales than the TES spatial resolution (Keppel-Aleks et al., 2011, 2012). Consequently, we conclude that part of the observed correlation is due to transport of nearby emissions into the plume.

In addition to the agreement with the slopes of the TES and GEOS-Chem CH_4/CO distributions, the RMS of the differences between the TES CH_4 observations and the VMRs of methane from the GEOS-Chem model (Fig. 7c) is 14.8 ppb which is consistent with the mean TES observation error of 12.0 ppb Consequently, these "top-down" comparisons between the TES satellite observations of CH_4 and CO with those from GEOS-Chem provide confidence in the total methane emissions from Indonesia during this time period.

5.2 South American fire plume

The distribution of CH_4 and CO for air parcels affected by the South American fire plumes are shown in Fig. 10. Only data over land between −30° S and

ACPD
12, 26207–26243, 2012

−10° S and −70° E through −40° E are used. The slope of CH_4 versus CO is 0.47 (ppb ppb^{-1}) ± 0.04 for the TES data. The slope is 0.47 (ppb ppb^{-1}) ± 0.02 for the GEOS-Chem model estimates. The larger slopes, as compared to the slope of the CH_4/CO distribution from Indonesia, indicate that wetlands emissions (or other non-fire emissions as shown in Table 1) are the primary contributors to the methane distribution for the observed air parcels. This conclusion is supported by the observed CH_4 values larger than 1800 ppb for the lower CO values of approximately 90 ppb which are not expected from the GEOS-Chem model and are well above the distribution of CH_4 values in the linear fit to the TES CH_4/CO distribution In addition, Table 1 (middle column) indicates that biomass burning emission of methane are much smaller than other emissions.

We again performed a sensitivity test in which the methane emissions from biomass burning were set to zero for the September through November time period in GEOS-Chem. The modeled slope for the CH_4/CO distributions was reduced from 0.47 to 0.44 and the correlation was reduced to 0.81. This 0.03 difference can be compared to the emission ratio of approximately 0.05 (g g^{-1}) or 0.088 molecules of CH_4 per molecule of CO for the fire emissions used in this GEOS-Chem model. The mismatch in the reduction of the slope is due to scatter in the modeled CH_4 and CO distributions. From this analysis, we conclude that the correlation between CO and CH_4 is primarily driven by transport of nearby wetlands emissions or other sources (e.g. livestock) into the observed air parcels.

Because wetlands and livestock (or other non-fire emissions) are the primary contributors to the distribution of CH_4 over this region (middle column Table 1) it is more difficult to place direct constraints on the total methane emissions and those due to biomass burning for this region and for this time period. However, this analysis suggests that CO might be a useful transport tracer for placing constraints on total methane emissions as demonstrated for CO_2 fluxes (e.g. Palmer et al., 2006; Wang et al., 2009). Alternatively, observations in the change of the slope of the CH_4/CO distribution over "short" time periods might provide constraints on biomass burning over this region if

ACPD
12, 26207–26243, 2012

we assume that non-fire emissions remain approximately constant over the "short" time period. We will test these approaches in subsequent research.

5.3 Southern African fire plumes

The distribution of CH_4 and CO for the air parcels affected by the African fire plumes are shown in Fig. 11. Only data between −30° S and −10° S and 10° E through 45° E are used. The slope for the TES CH_4/CO distribution is 0.44 (ppb ppb^{-1}) ± 0.03 with a correlation of R = 0.42 The slope for CH_4/CO distribution from GEOS-Chem is 0.46 (ppb ppb^{-1}) ± 0.03 for the average tropospheric model estimates. The fact that the differences between TES and GEOS-Chem are larger than the mean observation error in each grid box also indicates that the sources of these methane and CO enhancements are not well quantified. Subsequent analysis and data will be needed to place constraints on the methane budget in this region.

6 Summary

In this paper we use new free-tropospheric CH_4 observations from the Aura TES satellite instrument to place constraints on methane emissions from tropical fires during the 2006 El Niño when there were strong peat fires over Indonesia as well as fires over South America and Southern Africa. We first evaluated the global distribution of free tropospheric CH_4 and CO from Aura TES observations against the GEOS-Chem model for October 2006. We find that the TES CH_4 is biased high relative to the GEOS-Chem CH_4 distributions by approximately 26.3 ppb, consistent with previous validation studies involving the HIPPO aircraft campaign (Wecht et al., 2012). This bias is nearly uniform for latitudes between 50° S and 80° N; higher biases south of 50° S are likely a result of inconsistencies in the tropopause height between the TES and GEOS-Chem stratospheric CH_4 distributions.

ACPD
12, 26207–26243, 2012

We find that the slopes of the TES and GEOS-Chem CH_4/CO distributions for the Indonesian peat fires and over South America and Southern Africa (30° S to 10° S) are consistent (within the error of the slope). In addition, the TES methane observations and the GEOS-Chem methane distributions are consistent (within the TES data uncertainty) for air parcels affected by the Indonesian peat fire plumes. We therefore conclude that the relative distribution of emissions from fires versus biotic emissions in GEOS-Chem is robust, that is, modeled distributions are within the uncertainties of the TES observations. Over Indonesia, an observed slope of 0.13 (ppb ppb^{-1}) ± 0.01, as compare to a modeled slope of 0.15 (ppb ppb^{-1}) ± 0.005 and an emission ratio of 0.11, indicate that most of the observed methane in the fire plumes over Indonesia came from the fires. A sensitivity study in which biomass burning emissions of methane are turned off in GEOS-Chem supports this conclusion because the modeled (no methane from biomass burning) CH_4/CO distribution becomes 0.045 (ppb ppb^{-1}) ± 0.005. However this sensitivity study also indicates that a component of this distribution is due to transport of non-fire emissions into the observed plume. Finally, Laboratory measurements of peat fire plumes (Christian et al., 2003) have an emission ratio of approximately 0.18 which is much larger than the emission ratio used in this study, indicating that the fires plumes have a combination of peat and non-peat sources. Because we can attribute most of the enhanced methane in these Indonesian fire plume to the actual fire and not from other emissions, it is likely that we can place direct constraints on the methane emissions from the fire using estimates of CO emissions such as might be obtained from the near surface CO estimates from the TERRA MOPITT satellite (e.g. Worden et al., 2010); this will be the subject of a subsequent study.

Unlike the Indonesian CH_4/CO distributions, the slopes of the air parcels affected by fire plumes over South America and Southern African regions are much larger (Slopes ~ 0.47 ± 0.04 and 0.44 ± 0.03, respectively, units of ppb ppb^{-1}) than the slope expected from biomass burning alone even though the CH_4 and CO distributions are correlated (R ~ 0.46 and 0.42, respectively). By conducting a sensitivity study in which biomass burning sources of methane were "turned off" in the GEOS-Chem model

ACPD
12, 26207–26243, 2012

during the observation time frame, we conclude that transport of nearby biotic (e.g. wetlands and livestock) emissions into the observed air parcels are the primary contributor to atmospheric CH_4 in these observed air parcels Further investigation is therefore needed to better constrain fire-based methane emissions over these regions during this time period. For example, changes in the observed CH_4/CO slope during peak fire season might be useful for placing constraints on methane emissions from these fires. We will also test whether CO can be used as a transport tracer to constrain CH_4 emissions as studied for CO_2 fluxes by Palmer et al. (2006) and Wang et al. (2009).

Acknowledgements. Part of this research was carried out at the Jet Propulsion Laboratory, California Institute of Technology, under a contract with the National Aeronautics and Space Administration. The authors would like to thank Peter Bergamaschi for providing TM5 CH_4 distributions which helped to initiate this analysis.

References

Andreae, M. O. and Merlet, P.: Emission of trace gases and aerosols from biomass burning, Global Biogeochem. Cy., 15, 955–966, 2001.

Beer, R., Glavich, T. A., and Rider, D. M.: Tropospheric emission spectrometer for the Earth Observing System's Aura satellite, Appl. Optics, 40, 2356–2367, 2001.

Bey, I., Jacob, D., Yantosca, R., Logan, J., Field, B., Fiore, A., Li, Q., Liu, H. Y., Mickley, L., and Schultz, M. G.: Global modeling of tropospheric chemistry with assimilated meteorology: model description and evaluation, J. Geophys. Res.-Atmos., 106, 23073–23095, 2001.

Bloom, A. A., Palmer, P. I., Fraser, A., Reay, D. S., and Frankenberg, C.: Large-scale controls of methanogenesis inferred from methane and gravity spaceborne data, Science, 327, 322–325, doi:10.1126/science.1175176, 2010.

Bousquet, P., Ciais, P., Miller, J. B., Dlugokencky, E. J., Hauglustaine, D. A., Prigent, C., Van Der Werf, G. R., Peylin, P., Brunke, E.-G., Carouge, C., Langenfelds, R. L., Lathière, J., Papa, F., Ramonet, M., Schmidt, M., Steele, L. P., Tyler, S. C., and White, J.: Contribution of anthropogenic and natural sources to atmospheric methane variability, Nature, 443, 439–443, doi:10.1038/nature05132, 2006.

ACPD

12, 26207–26243, 2012

Bousquet, P., Ringeval, B., Pison, I., Dlugokencky, E. J., Brunke, E.-G., Carouge, C., Chevallier, F., Fortems-Cheiney, A., Frankenberg, C., Hauglustaine, D. A., Krummel, P. B., Langenfelds, R. L., Ramonet, M., Schmidt, M., Steele, L. P., Szopa, S., Yver, C., Viovy, N., and Ciais, P.: Source attribution of the changes in atmospheric methane for 2006–2008, Atmos. Chem. Phys., 11, 3689–3700, doi:10.5194/acp-11-3689-2011, 2011.

Bowman, K. W., Rodgers, C. D., Kulawik, S. S., Worden, J., Sarkissian, E., Osterman, G., Steck, T., Lou, M., Eldering, A., Shephard, M., Worden, H., Lampel, M., Clough, S., Brown, P., Rinsland, C., Gunson, M., and Beer, R.: Tropospheric emission spectrometer: retrieval method and error analysis, IEEE T. Geosci. Rem., 44, 1–11, doi:10.1109/TGRS.2006.871234, 2006.

Christian, T. J.: Comprehensive laboratory measurements of biomass-burning emissions: 1. Emissions from Indonesian, African, and other fuels, J. Geophys. Res., 108, D234719, doi:10.1029/2003JD003704, 2003.

Clough, S. A., Shephard, M. W., Worden, J., Brown, P. D., Worden, H. M., Luo, M., Rodgers, C. D., Rinsland, C. P., Goldman, A., and Brown, L.: Forward model and Jacobians for tropospheric emission spectrometer retrievals, IEEE T. Geosci. Rem., 44, 1308–1323, 2006.

Crevoisier, C., Nobileau, D., Fiore, A. M., Armante, R., Chédin, A., and Scott, N. A.: Tropospheric methane in the tropics – first year from IASI hyperspectral infrared observations, Atmos. Chem. Phys., 9, 6337–6350, doi:10.5194/acp-9-6337-2009, 2009.

Deeter, M. N., Worden, H. M., Gille, J. C., Edwards, D. P., Mao, D., and Drummond, J. R.: MOPITT multispectral CO retrievals: origins and effects of geophysical radiance errors, J. Geophys. Res., 116, D15303, doi:10.1029/2011JD015703, 2011.

Deeter, M. N., Worden, H. M., Edwards, D. P., Gille, J. C., and Andrews, A. E.: Evaluation of MOPITT retrievals of lower-tropospheric carbon monoxide over the United States, J. Geophys. Res., 117, D13306, doi:10.1029/2012JD017553, 2012.

Denman, K. L., Brasseur, G., Chidthaisong, A., Ciais, P., Cox, P. M., Dickinson, R. E., Hauglustaine, D., Heinze, C., Holland, E., Jacob, D., Lohmann, U., Ramachandran, S., da Silva Dias, P. L., Wofsy, S. C., and Zhang, X.: Couplings between changes in the climate system and biogeochemistry, in: Climate Change 2007: The Physical Science Basis, Contribution of Working Group I to the Fourth Assessment Report of the Intergovernmental Panel on Climate Change, edited by: Solomon, S., Qin, D., Manning, M., Chen, Z., Marquis, M., Averyt, K. B., Tignor, M., and Miller, H. L., 501–587, Cambridge University Press, Cambridge, UK, 2007.

ACPD
12, 26207–26243, 2012

Dlugokencky, E., Masarie, K., Lang, P., Tans, P., Steele, L., and Nisbet, E.: A dramatic decrease in the growth rate of atmospheric methane in the Northern Hemisphere during 1992, Geophys. Res. Lett., 21, 43–43, 1994a.

Dlugokencky, E., Steele, L., Lang, P., and Masarie, K.: The growth rate and distribution of atmospheric methane, J. Geophys. Res., 99, 17021–17043, 1994b.

Dlugokencky, E. J., Bruhwiler, L., White, J. W. C., Emmons, L. K., Novelli, P. C., Montzka, S. A., Masarie, K. A., Lang, P. M., Crotwell, A. M., Miller, J. B., and Gatti, L. V.: Observational constraints on recent increases in the atmospheric CH_4 burden, Geophys. Res. Lett., 36, L18803, doi:10.1029/2009GL039780, 2009.

Dlugokencky, E. J., Nisbet, E. G., Fisher, R., and Lowry, D.: Global atmospheric methane: budget, changes and dangers, Philos. Trans. R. Soc. A, 369, 2058–2072, doi:10.1098/rsta.2010.0341, 2011.

Eldering, A., Kulawik, S. S., Worden, J., Bowman, K., and Osterman, G.: Implementation of cloud retrievals for TES atmospheric retrievals: 2. Characterization of cloud top pressure and effective optical depth retrievals, J. Geophys. Res., 113, D16S37, doi:10.1029/2007JD008858, 2008.

European Commission, Joint Research Centre (JRC)/Netherlands Environmental Assessment Agency (PBL): Emission Database for Global Atmospheric Research (EDGAR), release version 4.0, available at: http://edgar.jrc.ec.europa.eu, (last access: 28 September 2012), 2009.

Forster, P., Ramaswamy, V., Artaxo, P., Berntsen, T., Betts, R., Fahey, D. W., Haywood, J., Lean, J., Lowe, D. C., Myhre, G., Nganga, J., Prinn, R., Raga, G., Schulz, M., and Van Dorland, R.: Changes in atmospheric constituents and in radiative forcing, in: Climate Change 2007: The Physical Science Basis, Contribution of Working Group I to the Fourth Assessment Report of the Intergovernmental Panel on Climate Change, edited by: Solomon, S., Qin, D., Manning, M., Chen, Z., Marquis, M., Averyt, K. B., Tignor, M., and Miller, H. L., Cambridge University Press, Cambridge, UK and New York, NY, USA, 2007.

Frankenberg, C., Meirink, J., Van Weele, M., Platt, U., and Wagner, T.: Assessing methane emissions from global space-borne observations, Science, 308, 1010–1014, doi:10.1126/science.1106644, 2005.

Frankenberg, C., Aben, I., Bergamaschi, P., Dlugokencky, E. J., van Hees, R., Houweling, S., van der Meer, P., Snel, R., and Tol, P.: Global column-averaged methane mixing ratios from 2003 to 2009 as derived from SCIAMACHY: trends and variability, J. Geophys. Res., 116, D04302, doi:10.1029/2010JD014849, 2011.

ACPD
12, 26207–26243, 2012

Fung, I., Prather, M., John, J., Lerner, J., and Matthews, E.: Three-dimensional model synthesis of the global methane cycle, J. Geophys. Res., 96, 13033–13065, 1991.
Gonzi, S. and Palmer, P. I.: Vertical transport of surface fire emissions observed from space, J. Geophys. Res., 115, D02306, doi:10.1029/2009JD012053, 2010.
Ho, S.-P., Edwards, D. P., Gille, J. C., Luo, M., Osterman, G. B., Kulawik, S. S., and Worden, H.: A global comparison of carbon monoxide profiles and column amounts from Tropospheric Emission Spectrometer (TES) and Measurements of Pollution in the Troposphere (MOPITT), J. Geophys. Res., 114, D21307, doi:10.1029/2009JD012242, 2009.
Kaplan, J. O.: Wetlands at the Last Glacial Maximum: distribution and methane emissions, Geophys. Res. Lett., 29, 1079, doi:10.1029/2001GL013366, 2002.
Keppel-Aleks, G., Wennberg, P. O., and Schneider, T.: Sources of variations in total column carbon dioxide, Atmos. Chem. Phys., 11, 3581–3593, doi:10.5194/acp-11-3581-2011, 2011.
Keppel-Aleks, G., Wennberg, P. O., Washenfelder, R. A., Wunch, D., Schneider, T., Toon, G. C., Andres, R. J., Blavier, J.-F., Connor, B., Davis, K. J., Desai, A. R., Messerschmidt, J., Notholt, J., Roehl, C. M., Sherlock, V., Stephens, B. B., Vay, S. A., and Wofsy, S. C.: The imprint of surface fluxes and transport on variations in total column carbon dioxide, Biogeosciences, 9, 875–891, doi:10.5194/bg-9-875-2012, 2012.
Kulawik, S. S., Worden, J., Eldering, A., Bowman, K., Gunson, M., Osterman, G. B., Zhang, L., Clough, S. A., Shephard, M. W., and Beer, R.: Implementation of cloud retrievals for Tropospheric Emission Spectrometer (TES) atmospheric retrievals: part 1. Description and characterization of errors on trace gas retrievals, J. Geophys. Res., 111, D24204, doi:10.1029/2005JD006733, 2006.
Lelieveld, J., Crutzen, P. J., and Dentener, F. J.: Changing concentration, lifetime and climate forcing of atmospheric methane, Tellus, 50, 128–150, 1998.
Logan, J. A., Megretskaia, I., Nassar, R., Murray, L. T., Zhang, L., Bowman, K. W., Worden, H. M., and Luo, M.: Effects of the 2006 El Niño on tropospheric composition as revealed by data from the Tropospheric Emission Spectrometer (TES), Geophys. Res. Lett., 35, L03816, doi:10.1029/2007GL031698, 2008.
Luo, M., Rinsland, C., Fisher, B., Sachse, G., Diskin, G., Logan, J., Worden, H., Kulawik, S., Osterman, G., Eldering, A., Herman, R., and Shephard, M.: TES carbon monoxide validation with DACOM aircraft measurements during INTEX-B 2006, J. Geophys. Res., 112, D24S48, doi:10.1029/2007JD008803, 2007.

ACPD
12, 26207–26243, 2012

Luo, M., Boxe, C., Jiang, J., Nassar, R., and Livesey, N.: Interpretation of Aura satellite observations of CO and aerosol index related to the December 2006 Australia fires, Remote Sens. Environ., 114, 2853–2862, doi:10.1016/j.rse.2010.07.003, 2010.

Nassar, R., Logan, J. A., Megretskaia, I. A., Murray, L. T., Zhang, L., and Jones, D. B. A.: Analysis of tropical tropospheric ozone, carbon monoxide, and water vapor during the 2006 El Niño using TES observations and the GEOS-Chem model, J. Geophys. Res., 114, D17304, doi:10.1029/2009JD011760, 2009.

O'Connor, F. M., Boucher, O., Gedney, N., Jones, C. D., Folberth, G. A., Coppell, R., Friedlingstein, P., Collins, W. J., Chappellaz, J., Ridley, J., and Johnson, C. E.: Possible role of wetlands, permafrost, and methane hydrates in the methane cycle under future climate change: a review, Rev. Geophys., 48, RG4005, doi:10.1029/2010RG000326, 2010.

Palmer, P. I., Suntharalingam, P., Jones, D. B. A., Jacob, D. J., Streets, D. G., Fu, Q., Vay, S. A., and Sachse, G. W.: Using CO_2 : CO correlations to improve inverse analyses of carbon fluxes, J. Geophys. Res., 111, D12318, doi:10.1029/2005JD006697, 2006.

Page, S. E., Siegert, F., Rieley, J. O., Boehm, H. D. V., Jaya, A., and Limin, S.: The amount of carbon released from peat and forest fires in Indonesia during 1997, Nature, 420, 61–65, 2002.

Park, R. J., Jacob, D. J., Field, B. D., Yantosca, R. M., and Chin, M.: Natural and transboundary pollution influ- ences on sulfate-nitrate-ammonium aerosols in the United States: implications for policy, J. Geophys. Res., 109, D15204, doi:10.1029/2003JD004473, 2004.

Pétron, G., Frost, G. J., Miller, B. R., Hirsch, A. I., Montzka, S. A., Karion, A., Trainer, M. K., Sweeney, C., Andrews, A. E., Miller, L., Kofler, J., Bar-Ilan, A., Dlugokencky, E. J., Patrick, L., Moore Jr., C. T., Ryerson, T. B., Siso, C., Kolodzey, W., Lang, P. M., Conway, T. J., Novelli, P. C., Masarie, K. A., Hall, B. D., Guenther, D., Kitzis, D. R., Miller, J. B., Welsh, D. C., Wolfe, D. E., Neff, W. D., and Tans, P. P.: Hydrocarbon emissions characterization in the Colorado Front Range – a pilot study, J. Geophys. Res., 117, D04304, doi:10.1029/2011JD016360, 2012.

Pickett-Heaps, C. A., Jacob, D. J., Wecht, K. J., Kort, E. A., Wofsy, S. C., Diskin, G. S., Worthy, D. E. J., Kaplan, J. O., Bey, I., and Drevet, J.: Magnitude and seasonality of wetland methane emissions from the Hudson Bay Lowlands (Canada), Atmos. Chem. Phys., 11, 3773–3779, doi:10.5194/acp-11-3773-2011, 2011.

Prinn, R. G., Huang, J., Weiss, R. F., Cunnold, D. M., Fraser, P. J., Simmonds, P. G., McCulloch, A., Harth, C., Reimann, S., Salameh, P., O'Doherty, S., Wang, R. H. J., Porter, L. W.,

ACPD
12, 26207–26243, 2012

Miller, B. R., and Krummel, P. B.: Evidence for variability of atmospheric hydroxyl radicals over the past quarter century, Geophys. Res. Lett., 32, L07809, doi:10.1029/2004GL022228, 2005.

Rigby, M., Prinn, R. G., Fraser, P. J., Simmonds, P. G., Langenfelds, R. L., Huang, J., Cunnold, D. M., Steele, L. P., Krummel, P. B., Weiss, R. F., O'doherty, S., Salameh, P. K., Wang, H. J., Harth, C. M., Mühle, J., and Porter, L. W.: Renewed growth of atmospheric methane, Geophys. Res. Lett., 35, L22805, doi:10.1029/2008GL036037, 2008.

Shindell, D., Kuylenstierna, J. C. I., Vignati, E., Van Dingenen, R., Amann, M., Klimont, Z., Anenberg, S. C., Muller, N., Janssens-Maenhout, G., Raes, F., Schwartz, J., Faluvegi, G., Pozzoli, L., Kupiainen, K., Hoglund-Isaksson, L., Emberson, L., Streets, D., Ramanathan, V., Hicks, K., Oanh, N. T. K., Milly, G., Williams, M., Demkine, V., and Fowler, D.: Simultaneously mitigating near-term climate change and improving human health and food security, Science, 335, 183–189, doi:10.1126/science.1210026, 2012.

Verma, S., Worden, J., Pierce, B., Jones, D. B. A., Al-Saadi, J., Boersma, F., Bowman, K., Eldering, A., Fisher, B., Jourdain, L., Kulawik, S., and Worden, H.: Ozone production in boreal fire smoke plumes using observations from the Tropospheric Emission Spectrometer and the Ozone Monitoring Instrument, J. Geophys. Res., 114, D02303, doi:10.1029/2008JD010108, 2009.

van der Werf, G. R., Randerson, J. T., Giglio, L., Collatz, G. J., Kasibhatla, P. S., and Arellano Jr., A. F.: Interannual variability in global biomass burning emissions from 1997 to 2004, Atmos. Chem. Phys., 6, 3423–3441, doi:10.5194/acp-6-3423-2006, 2006.

van der Werf, G. R., Randerson, J. T., Giglio, L., Collatz, G. J., Mu, M., Kasibhatla, P. S., Morton, D. C., DeFries, R. S., Jin, Y., and van Leeuwen, T. T.: Global fire emissions and the contribution of deforestation, savanna, forest, agricultural, and peat fires (1997–2009), Atmos. Chem. Phys., 10, 11707–11735, doi:10.5194/acp-10-11707-2010, 2010.

van Leeuwen, T. T. and van der Werf, G. R.: Spatial and temporal variability in the ratio of trace gases emitted from biomass burning, Atmos. Chem. Phys., 11, 3611-3629, doi:10.5194/acp-11-3611-2011, 2011.

Wang, J. S., Logan, J. A., McElroy, M. B., Duncan, B. N., Megretskaia, I. A., and Yantosca, R. M.:, A 3-D model analysis of the slowdown and interannual variability in the methane growth rate from 1988 to 1997, Global Biogeochem. Cy., 18, GB3011, doi:10.1029/2003GB002180, 2004.

ACPD
12, 26207–26243, 2012

Wang, H., Jacob, D. J., Kopacz, M., Jones, D. B. A., Suntharalingam, P., Fisher, J. A., Nassar, R., Pawson, S., and Nielsen, J. E.: Error correlation between CO_2 and CO as constraint for CO_2 flux inversions using satellite data, Atmos. Chem. Phys., 9, 7313–7323, doi:10.5194/acp-9-7313-2009, 2009.

Wecht, K. J., Jacob, D. J., Wofsy, S. C., Kort, E. A., Worden, J. R., Kulawik, S. S., Henze, D. K., Kopacz, M., and Payne, V. H.: Validation of TES methane with HIPPO aircraft observations: implications for inverse modeling of methane sources, Atmos. Chem. Phys., 12, 1823–1832, doi:10.5194/acp-12-1823-2012, 2012.

Worden, J., Kulawik, S., Shephard, M., Clough, S., Worden, H., Bowman, K., and Goldman, A.: Predicted errors of tropospheric emission spectrometer nadir retrievals from spectral window selection, J. Geophys. Res., 109, D09308, doi:10.1029/2004JD004522, 2004.

Worden, H. M., Deeter, M. N., Edwards, D. P., Gille, J. C., Drummond, J. R., and Nedelec, P.: Observations of near-surface carbon monoxide from space using MOPITT multispectral retrievals, J. Geophys. Res., 115, D18314, doi:10.1029/2010JD014242, 2010.

Worden, J., Kulawik, S., Frankenberg, C., Payne, V., Bowman, K., Cady-Peirara, K., Wecht, K., Lee, J.-E., and Noone, D.: Profiles of CH_4, HDO, H_2O, and N_2O with improved lower tropospheric vertical resolution from Aura TES radiances, Atmos. Meas. Tech., 5, 397–411, doi:10.5194/amt-5-397-2012, 2012.

ACPD
12, 26207–26243, 2012

Table 1. CH_4 emissions used for 2006 GEOS-Chem model estimates for October 2006.

Emission type	CH_4 emissions ($Tg\,month^{-1}$)		
	Indonesia 15° S–5° N	South America 10° S–30° S	Southern Africa 10° S–30° S
Total	4.063	3.229	0.938
Gas and Oil	0.203	0.082	0.018
Coal	0.031	0.004	0.096
Livestock	0.042	1.08	0.17
Waste	0.188	0.198	0.079
Biofuel	0.031	0.06	0.028
Rice	0.089	0.019	0.009
Other Anthro	0.004	0.005	0.002
Biomass	2.768	0.039	0.183
Wetlands	0.688	1.641	0.27
Soil abs.	0.001	0.03	0.054
Other natural	0.019	0.101	0.084

ACPD
12, 26207–26243, 2012

Table 2. CO emissions used for GEOS-Chem model estimates for October 2006.

Emission type	CO emissions (Tg month^{-1})		
	Indonesia 15° S–5° N	South America 10° S–30° S	Southern Africa 10° S–30° S
Total	45.191	2.658	5.954
Fossil fuel	1.285	0.533	0.322
Biomass	43.735	0.856	5.087
Biofuel	0	0.827	0.391
Monoterpene Oxidation	0.172	0.443	0.153

ACPD
12, 26207–26243, 2012

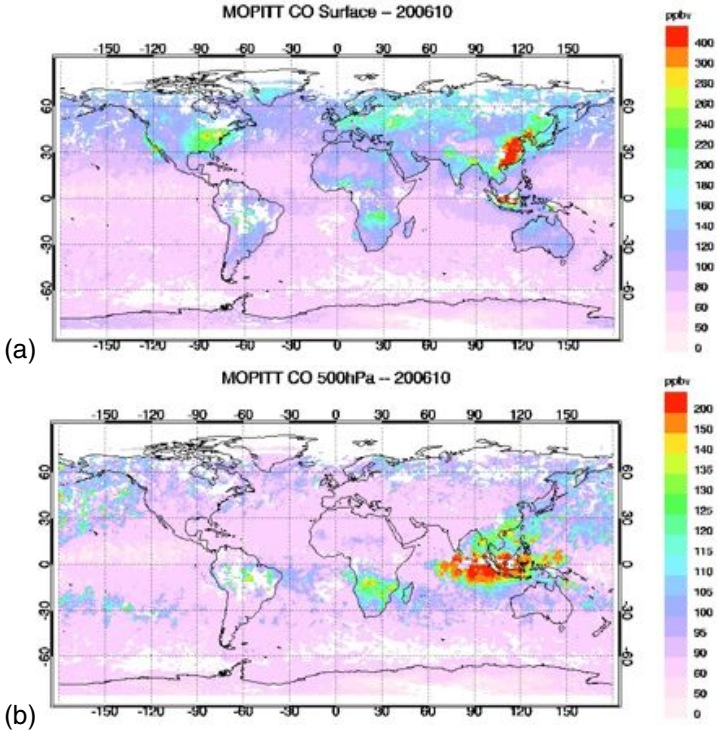

Fig. 1. (a) Surface CO estimates from the TERRA MOPITT satellite for October 2006. **(b)** Tropospheric CO estimates from the TERRA MOPITT satellite for October 2006.

ACPD
12, 26207–26243, 2012

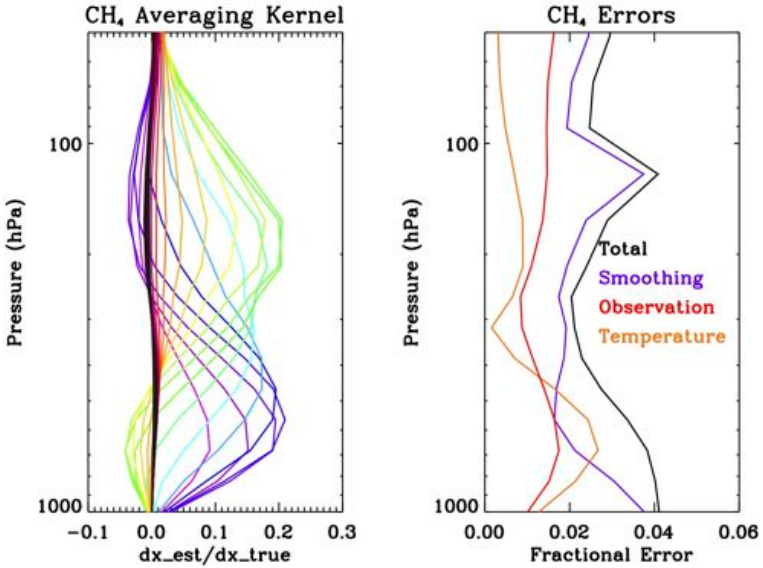

Fig. 2. (Left panel) Averaging kernels for TES estimate of CH_4 for tropical scene. Different colors help to distinguish pressures corresponding to each averaging kernel. (Right panel) Error distribution for TES CH_4 estimate for tropical scene. The observation error includes uncertainties from noise and interferences such as H_2O.

ACPD
12, 26207–26243, 2012

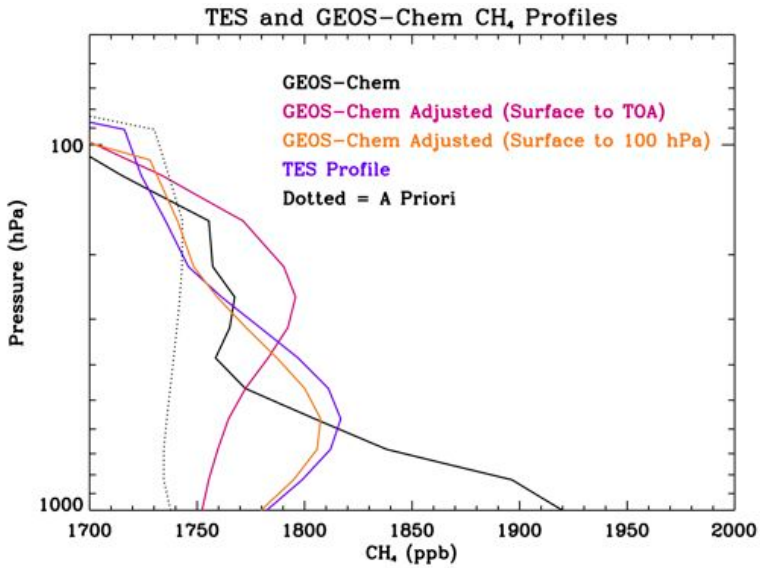

Fig. 3. Comparison of TES and GEOS-Chem profiles. (Black) GEOS-Chem CH_4 profile over S. America over region of enhanced biomass burning. The red line shows the GEOS-Chem profile after applying the TES constraint vector and full averaging kernel (from surface to the top-of-atmosphere). The orange line shows the GEOS-Chem profile if only the averaging kernels from the surface to 100 hPa are applied to the GEOS-Chem profile. The TES profile is shown in blue and the a priori is the dotted line.

ACPD
12, 26207–26243, 2012

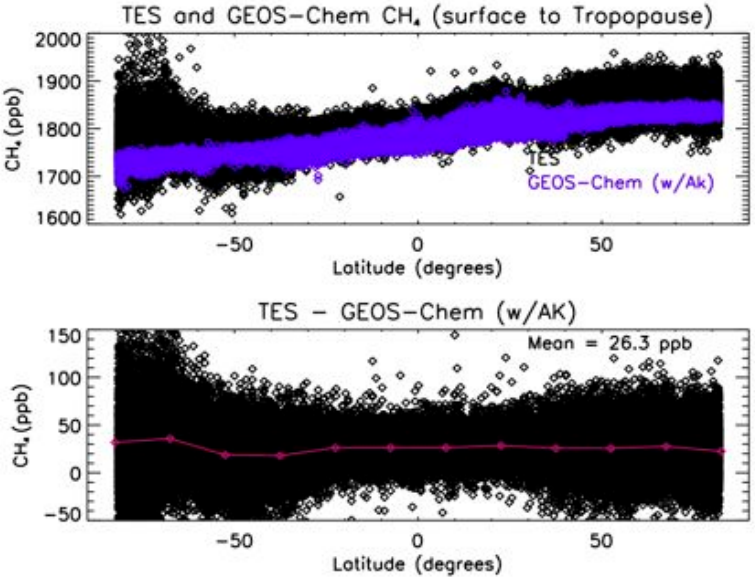

Fig. 4. (Top panel) Latitudinal distribution of TES October 2006 tropospheric CH_4 estimates (black diamonds), corresponding GEOS-Chem estimates adjusted with TES instrument operator (blue diamonds). (Bottom panel) Difference between TES and adjusted GEOS-Chem estimates (black – red from top panel). The red line in the bottom panel shows the mean difference between TES and the adjusted GEOS-Chem estimates when these differences are averaged for data within 15 degree latitude bins.

ACPD
12, 26207–26243, 2012

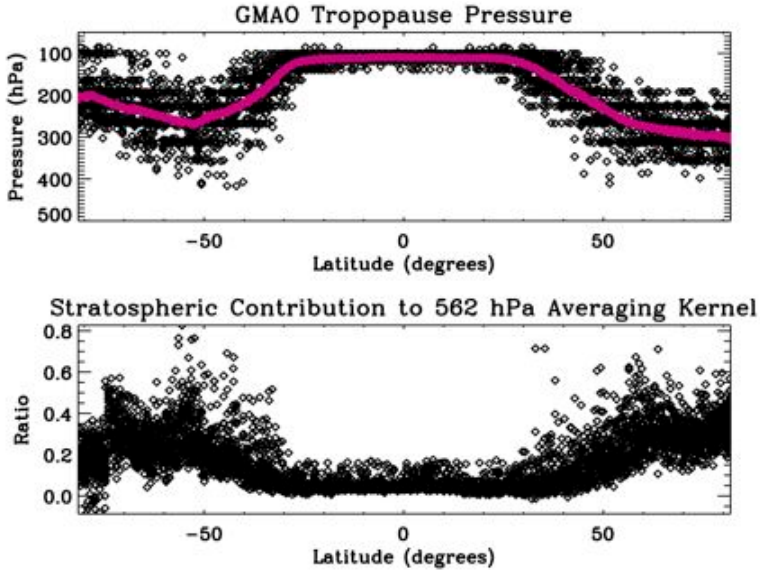

Fig. 5. (Top panel) Tropopause height from GMAO. The red line is the latitudinal average. (bottom panel) Contribution of stratospheric differences between TES a priori and "true" CH_4 distributions to the TES tropospheric CH_4 estimate at 562 hPa.

ACPD
12, 26207–26243, 2012

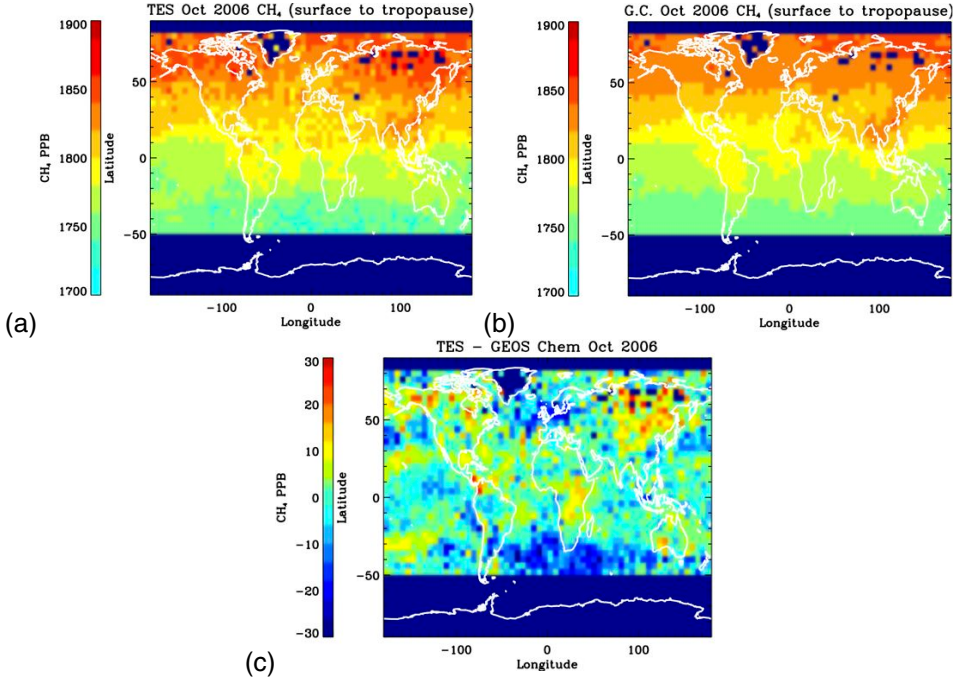

Fig. 6. (a) TES Tropospheric CH_4 estimates. The TES estimates have been reduced by 26.3 ppb. **(b)** Corresponding GEOS-Chem CH_4 estimates, adjusted with the TES instrument operator. **(c)** Difference between TES and GEOS-chem.

ACPD
12, 26207–26243, 2012

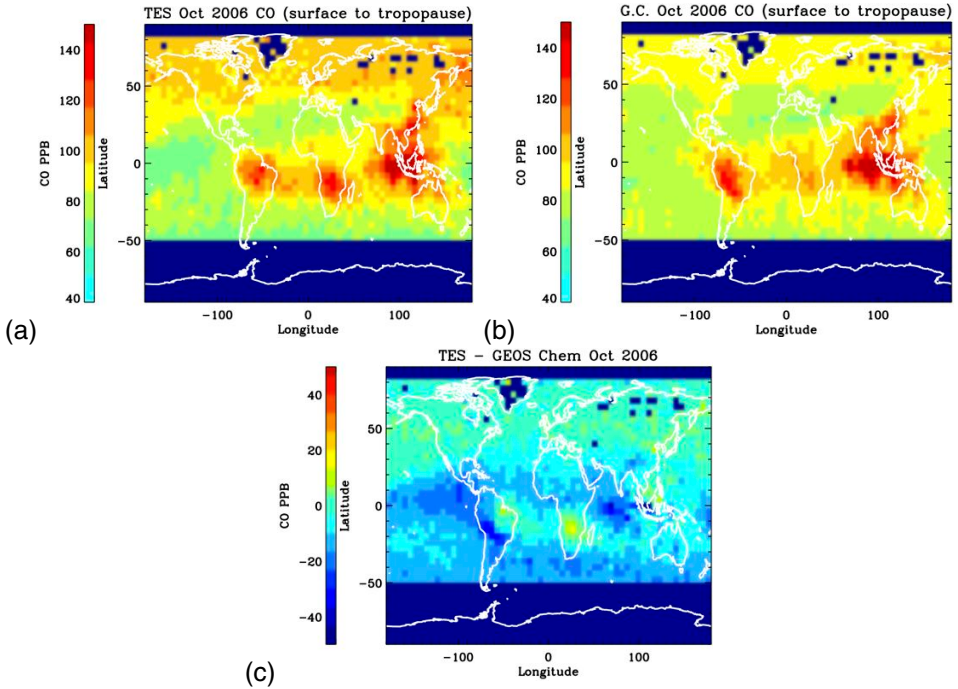

Fig. 7. (a) TES Tropospheric CO estimates. **(b)** Corresponding GEOS-Chem CO estimates, adjusted with the TES instrument operator. The GEOS-Chem values have been reduced by 19.9 ppb. **(c)** Difference between TES and GEOS-chem.

ACPD
12, 26207–26243, 2012

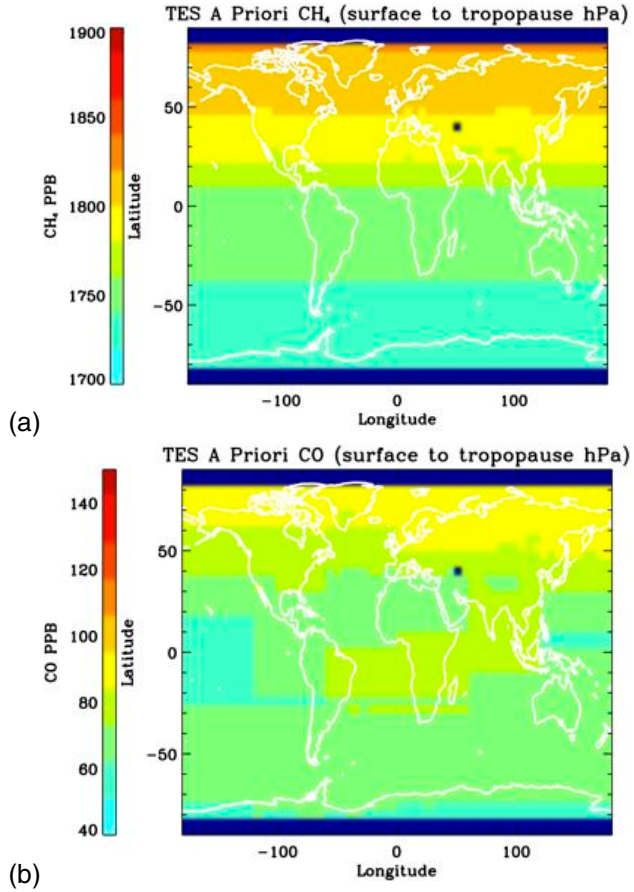

Fig. 8. (a) The TES CH_4 a priori, averaged over all pressure levels in the TES forward model in the troposphere. **(b)** Same as **(a)** but for CO.

ACPD
12, 26207–26243, 2012

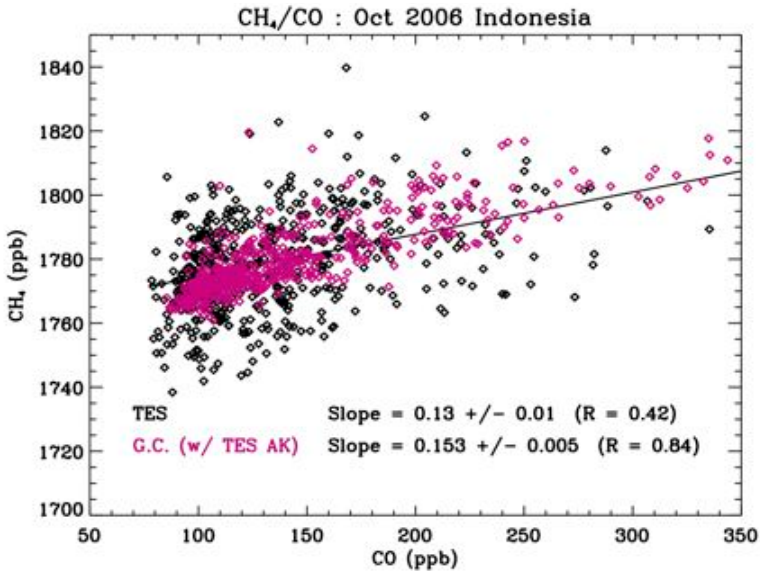

Fig. 9. Distribution of CH_4 and CO over Indonesian Fires. The TES data are shown in black. The GEOS-Chem data (adjusted with the TES operator) is in red. A linear fit to the TES data is shown as a black line.

ACPD
12, 26207–26243, 2012

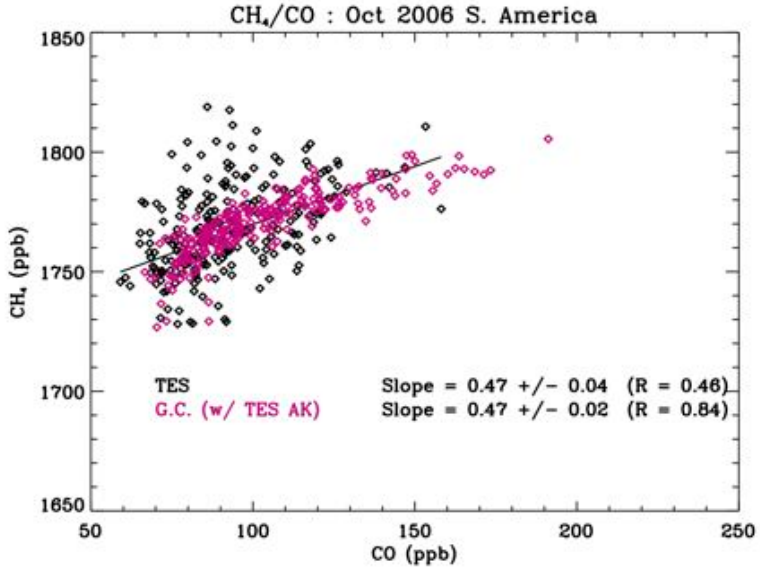

Fig. 10. Distribution of CH_4 and CO over South American Fires. The TES data are shown in black. The GEOS-Chem data (adjusted with the TES operator) is in red. A linear fit to the TES data is shown as a black line.

ACPD
12, 26207–26243, 2012

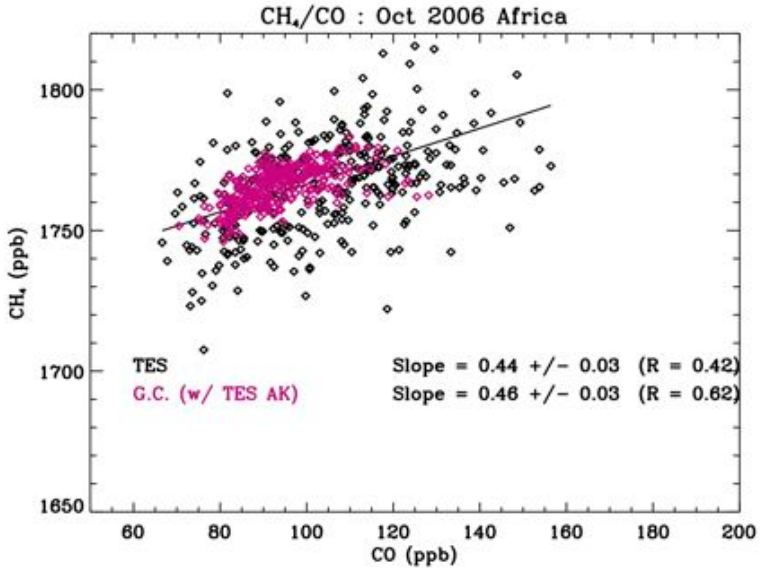

Fig. 11. Distribution of CH_4 and CO over African Fires. The TES data are shown in black. The GEOS-Chem data (adjusted with the TES operator) is in red. A linear fit to the TES data is shown as a black line.

ACPD
12, 26207–26243, 2012